Inorg. Chem. **2004**, *43*, 642–650

Generation of Spirotricyclic Site-Differentiated Cyclotriphosphazenes: A Solvent-Free Approach to Multidentate N/O Donor Ligand Systems

Michael Harmjanz,* Ingmar M. Piglosiewicz, Brian L. Scott, and Carol J. Burns

Chemistry Division, Los Alamos National Laboratory, MS J514, Los Alamos, New Mexico 87545

Received August 20, 2003

Cyclotriphosphazene-based ligand systems are valuable materials to model the metal-binding event on the structurally and electronically related functionalized high molecular weight polyphosphazenes. We here report the facile synthesis of novel spirotricyclic cyclotriphosphazenes $N_3P_3(MeNC_2H_4NMe)_2L_2$, $N_3P_3(iPrNC_2H_4NiPr)_2L_2$, and $N_3P_3(o\text{-}O_2C_{12}H_8)_2L_2$ that enables different substituents to be incorporated into the ligand system. This synthetic approach allows for control over the solubility and steric requirements of the exocyclic bidentate substituents, as well as the donor type and denticity of the coordination sites. A mononuclear lanthanum complex ($[La(NO_3)_3\{N_3P_3(pzpy)_2(MeNC_2H_4NMe)_2\}]$ (**7**)) and a series of dinuclear transition-metal complexes ($[\{ReCl(CO)_3\}_2\{N_3P_3(pyNH)_2(MeNC_2H_4NMe)_2\}]$ (**4**), $[\{FeI_2\}_2\{N_3P_3(pyNH)_2(MeNC_2H_4NMe)_2\}]$ (**5**), and $[\{PdCl_2\}_2\{N_3P_3(pyNH)_2(MeNC_2H_4NMe)_2]$ (**6**)) have been prepared and structurally and spectroscopically characterized to explore the metal coordination environments supported by this class of ligands.

Introduction

As witnessed by numerous applications, polyphosphazenes can incorporate an extraordinary combination of chemical properties through the judicious combination of side groups.[1,2] The ease with which metal-binding entities can be anchored in well-defined positions in close proximity is one of the most remarkable features of these polymeric materials with regard to metal complexation.

It is important to note that the functionalized phosphorus atoms of the low molecular weight cyclotriphosphazenes exhibit geometries and electronic properties related to those of the polymeric constructs (Chart 1). Consequently, metal binding at the macromolecules can be modeled with similar functionalized cyclotriphosphazenes. In addition, cyclophosphazene-based ligand systems are highly interesting metal-complexing agents in their own right.[3,4] While a number of cyclization reactions have been reported to produce functionalized cyclotriphosphazenes,[5] most synthetic routes start with the commercially available hexachlorocyclotriphosphazene ($N_3P_3Cl_6$). The derivatization of the phosphazene backbone can typically be accomplished via simple nucleophilic substitution reactions. Unfortunately, the incorporation of just one particular side group yields multidentate ligand constructs that often support multiple coordination modes or give rise to solution dynamic behavior of the resulting metal complexes.[6]

Chart 1. Structurally and Electronically Related Cyclotriphosphazenes (**I**) and Polyphosphazenes (**II**)

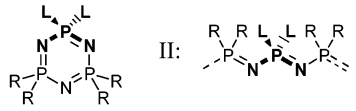

Since the simultaneous reaction of two or more substrates usually leads to complicated and intractable product mixtures, a reliable sequential substitution pathway is required to establish a well-defined, predictable coordination environment: two of the three phosphorus atoms of the cyclic phosphazene have to be blocked by noncoordinating substituents, with the remaining third isolated dichlorophosphorus unit being subjected to further substitution reactions. Although several examples of these 2:1-site-differentiated cyclotriphospha-

* Author to whom correspondence should be addressed. E-mail: mharm@lanl.gov.

(1) See, for example: (a) Gleria, M.; De Jaeger, R. *J. Inorg. Organomet. Polym.* **2001**, *11*, 1−45. (b) De Jaeger, R.; Gleria, M. *Prog. Polym. Sci.* **1998**, *23*, 179−276.
(2) Allcock, H. R. In *Phosphorus−Nitrogen Compounds*; Academic Press: New York and London, 1972.
(3) Chandrasekhar, V.; Thomas, K. R. J. *Appl. Organomet. Chem.* **1993**, *7*, 1−31 and references therein.
(4) See, e.g.: Allcock, H. R.; Desorcie, J. L.; Riding, G. H. *Polyhedron* **1987**, *6*, 119−157. Chandrasekhar V.; Krishnan, V. In *Advances in Inorganic Chemistry*; Sykes, A. G., Ed.; Academic Press: San Diego, CA, 2002; Vol. 53, pp 159−211.
(5) Wisian-Neilson, P.; Johnson, R. S.; Zhang, H.; Jung, J.-H.; Neilson, R. H.; Ji, J.; Watson W. H.; Krawiec, M. *Inorg. Chem.* **2002**, *41*, 4775−4779.
(6) Chandrasekhar, V.; Nagendran, S. *Chem. Soc. Rev.* **2001**, *30*, 193−203.

10.1021/ic034990b CCC: $27.50
Published on Web 12/25/2003

zenes exist,[7] current synthetic pathways to these materials often require multiple reaction steps or prolonged reaction times. We here report a straightforward procedure for the generation of highly flexible, cyclophosphazene-based ligand systems. This procedure involves a solvent-free reaction of the respective ligand with various site-differentiated dichlorocyclotriphosphazenes. A mononuclear lanthanum complex and several dinuclear transition-metal complexes have been prepared and structurally and spectroscopically characterized to demonstrate and evaluate the geometry of metal binding enabled by some of these ligand constructs.

Experimental Section

All manipulations have been carried out under an argon atmosphere. *N*,*N*′-Diisopropylethylenediamine, pyrazole, 3,5-dimethylpyrazole, 2-aminopyridine, 2,2′-dipyridylamine, 1,4-phenylenediamine, and 3,5-dimethylaniline were purchased from Aldrich and used as received. Hexachlorocyclotriphosphazene ($N_3P_3Cl_6$) and dichloro(1,5-cyclooctadiene)palladium [$PdCl_2$(COD)] were purchased from STREM. 2,2,-Dichloro-4,4,6,6-bis[spiro(*N*,*N*′-dimethylethylenediamino)]cyclotriphosphazene (**1**),[8] 2,2-dichloro-4,4,6,6-bis[spiro(2′,2″-dioxy-1′,1″-biphenylyl)]cyclotriphosphazene (**2**),[9] 3-(2-pyridyl)pyrazole,[10] 1,4,7,10-tetraoxa-13-azacyclopentadecane[11] and the metal complex [$ReCl(CH_3CN)_2(CO)_3$][12] were prepared as described in previously reported procedures.

Melt reactions were carried out under argon. The preparation and purification of the metal complexes **4** and **5** was carried out under a pure argon atmosphere with dry and degassed solvents using standard Schlenk techniques.

Microanalyses (C, H, and N) for all compounds were performed by the Micro-Mass Facility at the University of California, Berkeley. ^{1}H and ^{31}P{^{1}H} NMR spectra were recorded on a Varian Inova 300 MHz spectrometer (^{31}P, 121 MHz). The reported J_{PH}* (Hz) values refer to the strong (outer) doublet peaks of the signals (virtual coupling) observed in the ^{1}H NMR spectra of **1a**, **1c**, **1f**, and **4**. Electrochemical data were recorded using an electrochemical analyzer (CH-Instruments; CHI-software version 2.07) with platinum wire counter, platinum disk working, and silver wire reference electrodes.

Preparation of 2,2-Dichloro-4,4,6,6-bis[spiro(*N*,*N*′-diisopropylethylenediamino)]cyclotriphosphazene (2). A portion of $N_3P_3Cl_6$ (4.5 g, 12.9 mmol) was mixed with *N*,*N*′-diisopropylethylenediamine (25.0 g, 173.3 mmol). A white solid formed immediately, and the reaction mixture was heated to 140−150 °C for 3 h. A clear solution was formed upon heating. After the solution was cooled to room temperature, the brown mixture was washed with petroleum ether (40:60) (3 × 75 mL) and subsequently with CH_2Cl_2. The filtrate was evaporated to dryness and redissolved in 40 mL of MeOH. A 250 mL volume of water was added in small portions. After the resulting solution was stirred at room temperature for 1 h, the yellow precipitate was filtered, washed with water, and dried in vacuo. Recrystallization from heptane yielded 4.5 g of **2** (71%). ^{1}H NMR ($CDCl_3$): δ 3.40 (m, 4H), 3.09 (m, 8H), 1.15 (d, 12H, J = 6.7 Hz), 1.1 (d, 12H, J = 6.7 Hz). ^{31}P NMR ($CDCl_3$): δ 28.4 (t, J_{PP} = 53.1 Hz), 19.96 (d, J_{PP} = 53.1 Hz). Anal. Calcd for $C_{16}H_{36}N_7P_3Cl_2$: C, 39.19; H, 7.40; N, 20.00. Found: C, 39.22; H, 7.59; N, 19.99.

Preparation of 2,2-Dipyrazolyl-4,4,6,6-bis[spiro(*N*,*N*′-dimethylethylenediamino)]cyclotriphosphazene (1a). A portion of $N_3P_3Cl_2(MeNC_2H_4NMe)_2$ (**1**) (0.85 g, 2.25 mmol) was mixed with 5.00 g (73.44 mmol) of pyrazole. The mixture was refluxed for 3 h. The excess pyrazole was removed in vacuo on heating to 120 °C, and the residue was washed with hot cyclohexane (3 × 35 mL), yielding a yellow oil, which slowly solidified upon cooling. The residue was redissolved in CH_2Cl_2 and washed with water (3 × 15 mL). The organic solution was dried with Na_2SO_4 and evaporated to dryness. The white residue was dissolved in a minimum amount of hot THF, and slow addition of pentane afforded **1a** as a white crystalline material. Yield: 0.75 g (81%). ^{1}H NMR ($CDCl_3$): δ 7.97 (d, 2 H, J = 1.8 Hz), 7.76 (m, 2H), 6.33−6.32 (m, 2H), 3.18 (m, 8H, J_{PH}* = 11.1 Hz), 2.55 (m, 12 H, J_{PH}* = 12.3 Hz). ^{31}P NMR ($CDCl_3$): δ 28.3 (d, J_{PP} = 58.8 Hz), 6.8 (t, J_{PP} = 58.8 Hz). Anal. Calcd for $C_{14}H_{26}N_{11}P_3$: C, 38.10; H, 5.94; N, 34.91. Found: C, 38.00; H, 6.16; N, 34.61.

Preparation of 2,2-Dipyrazolyl-4,4,6,6-bis[spiro(*N*,*N*′-diisopropylethylenediamino)]cyclotriphosphazene (2a). A sample of $N_3P_3Cl_2(i\text{PrNC}_2H_4N i\text{Pr})_2$ (**2**) (1.00 g, 2.04 mmol) was mixed with solid pyrazole (7.50 g, 0.11 mol). The mixture was heated at reflux for 2 h. The excess pyrazole was removed in vacuo on heating to 120 °C, and the residue was dissolved in water. The aqueous solution was made basic by adding NH_3(aq) and subsequently extracted with CH_2Cl_2 (2 × 60 mL). The combined organic phases were washed with water (3 × 30 mL) and subsequently dried with Na_2SO_4. The solvent was evaporated under reduced pressure to afford **2a** as a white crystalline solid (1.04 g, 92%). ^{1}H NMR ($CDCl_3$): δ 7.99 (d, 2H, J = 2.7 Hz), 7.68 (dd, 2H, J_1 = J_2 = 1.6 Hz), 6.29−6.26 (m, 2 H), 3.43−3.33 (m, 4H), 3.15−3.09 (m, 8H), 1.11 (d, 12H, J = 6.6 Hz), 1.05 (d, 12H, J = 6.6 Hz). ^{31}P NMR ($CDCl_3$): δ 23.2 (d, J_{PP} = 57.1 Hz), 6.8 (t, J_{PP} = 57.1 Hz). Anal. Calcd for $C_{22}H_{42}N_{11}P_3$: C, 47.73; H, 7.65; N, 27.83. Found: C, 47.92; H, 7.80; N, 27.55.

Preparation of 2,2-Dipyrazolyl-4,4,6,6-bis[spiro(2′,2″-dioxy-1′,1″-biphenylyl)]cyclotriphosphazene (3a). A portion of $N_3P_3Cl_2$-(2,2′-$O_2C_{12}H_8)_2$ (**3**) (1.30 g, 2.26 mmol) was combined with solid pyrazole (8.00 g, 0.118 mol), and the mixture was refluxed for 2 h. Pyrazole was removed in vacuo on heating to 120 °C and the residue repeatedly washed with hot cyclohexane (3 × 60 mL). The remaining white solid was dissolved in CH_2Cl_2 (60 mL) and the organic phase washed with water (3 × 45 mL). The organic solution was dried (Na_2SO_4) and evaporated to dryness, leaving a solid residue, which was further purified by recrystallization from toluene. Yield: 1.18 g (82%). ^{1}H NMR ($CDCl_3$): δ 8.18 (d, 2H, J = 2.7 Hz), 7.80 (m, 2H), 7.52−7.23 (m, 16 H), 6.42−6.41 (m, 2H). ^{31}P NMR ($CDCl_3$): δ 23.8 (d, J_{PP} = 80.7 Hz), 4.7 (t, J_{PP} = 80.7 Hz). Anal. Calcd for $C_{30}H_{22}O_4N_7P_3$: C, 56.52; H, 3.48; N, 15.38. Found: C, 56.69; H, 3.58; N, 15.40.

Preparation of 2,2-Bis(3,5-dimethylpyrazolyl)-4,4,6,6-bis[spiro(2′,2″-dioxy-1′,1″-biphenylyl)]cyclotriphosphazene (3b). A portion of **3** (2.00 g, 3.48 mmol) was combined with solid 3,5-dimethylpyrazole (10.00 g, 0.104 mol). The mixture was heated to 190 °C and kept at this temperature for 7 h. After being cooled to room temperature, the reaction mixture was thoroughly washed with warm EtOH (3 × 20 mL). The solid residue was dried in vacuo and dissolved in 30 mL of CH_2Cl_2. The organic phase was washed with water (3 × 25 mL) and subsequently dried (Na_2SO_4). After

(7) (a) Chandrasekaran, A.; Krishnamurthy, S. S.; Nethaji, M. *J. Chem. Soc., Dalton Trans.* **1994**, 63-68. (b) Chandrasekaran, A.; Krishnamurthy, S. S.; Nethaji, M. *Inorg. Chem.* **1993**, *32*, 6102−6106. (c) Gallicano, K. D.; Paddock, N. L. *Can. J. Chem.* **1982**, *60*, 521−528.
(8) Chivers, T.; Hedgeland, R. *Can. J. Chem.* **1972**, *50*, 1017−1025.
(9) Dez, I.; De Jaeger, R. *Phosphorus, Sulfur, Silicon* **1997**, *130*, 1−14.
(10) Pleier, A. K.; Glas, H.; Grosche, M.; Sirsch, P.; Thiel, W. R. *Synthesis* **2001**, 55−62.
(11) Maeda, H.; Furuyoshi, S.; Nakatsuyi, Y.; Okahara, M. *Bull. Chem. Soc. Jpn.* **1983**, *56*, 3073−3077.
(12) Farona, M. F.; Kraus, K. F. *Inorg. Chem.* **1970**, *9*, 1700−1704.

removal of the solvents under reduced pressure, the white residue was dissolved in 10 mL of hot acetone, and addition of 60 mL of diethyl ether afforded **3b** as a crystalline solid. Yield: 1.4 g (58%). ^{1}H NMR ($CDCl_3$): δ 7.21−7.45 (m, 16H), 5.89 (d, 2H, J = 3.3 Hz), 2.32 (s, 6H) 2.18 (s, 6H). ^{31}P NMR ($CDCl_3$): δ 23.7 (d, J_{PP} = 80.8 Hz), 4.5 (t, J_{PP} = 80.8 Hz). Anal. Calcd for $C_{34}H_{30}O_4N_7P_3$: C, 58.88; H, 4.36; N, 14.14. Found: C, 59.06; H, 4.57; N, 14.04.

Preparation of 2,2-Bis(3-(2-pyridyl)pyrazolyl)-4,4,6,6-bis-[spiro(*N,N*′-dimethylethylenediamino)]cyclotriphosphazene (1c). A portion of **1** (2.00 g, 5.29 mmol) was combined with 3-(2-pyridyl)pyrazole (9.00 g, 62.00 mmol), and the mixture was heated to 200 °C for 3 h. The reaction mixture was allowed to cool to room temperature and repeatedly washed with hot water. The remaining white solid was dissolved in CH_2Cl_2 (40 mL), and the organic phase was washed with dilute aqueous ammonia and subsequently with water. The organic phase was dried with Na_2SO_4 and the solvent removed in vacuo. The residue was treated with 10 mL of acetone, yielding **1c** as a white crystalline solid (1.95 g, 62%). ^{1}H NMR ($CDCl_3$): δ 8.53 (d, 2 H, J = 4.5 Hz), 8.04 (d, 2H, J = 8.1 Hz), 7.91 (d, 2H, J = 2.7 Hz), 7.61 (dd, 2H, $J_1 = J_2$ = 7.6 Hz), 7.14 (dd, 2H, $J_1 = J_2$ = 6.2 Hz), 6.98 (t, 2H, J = 2.8 Hz), 3.13 (d, 8H, J_{PH}* = 9.9 Hz), 2.55 (d, 12H, J_{PH}* = 12.3 Hz). ^{31}P NMR ($CDCl_3$) δ 28.0 (d, J_{PP} = 58.8 Hz), 6.8 (t, J_{PP} = 58.8 Hz). Anal. Calcd for $C_{24}H_{32}N_{13}P_3$: C, 48.40; H, 5.42; N, 30.58. Found: C, 48.46; H, 5.57; N, 30.34.

Preparation of 2,2-Bis(3,5-dimethylphenylamino)-4,4,6,6-bis-[spiro(2′,2″-dioxy-1′,1″-biphenylyl)]cyclotriphosphazene (3d). A sample of **3** (1.270 g, 2.21 mmol) was suspended in 3,5-dimethylaniline (10.00 g, 82.5 mmol). The mixture was heated to 180 °C and kept at this temperature for 3 h. Excess amine was removed under vacuum, and the residue was thoroughly washed with petroleum ether (40:60). The remaining white solid was dissolved in 50 mL of CH_2Cl_2, and the organic phase was washed with diluted ammonia and water (2 × 30 mL). The organic phase was dried with Na_2SO_4 and evaporated to dryness. The residue was again washed with petroleum ether and recrystallized from toluene. Yield: 1.60 g (97%). ^{1}H NMR ($CDCl_3$): δ 7.46−7.45 (m, 4 H), 7.30−7.18 (m, 8H), 7.09−7.07 (m, 4H), 6.70 (s, 4H), 6.56 (s, 2H), 5.07 (d, 2H, J_{PH} = 9.0 Hz), 2.18 (s, 12H). ^{31}P NMR ($CDCl_3$): δ 26.2 (d, J_{PP} = 73.1 Hz), 6.5 (t, J_{PP} = 73.1 Hz). Anal. Calcd for $C_{40}H_{36}N_5O_4P_3$: C, 64.60; H, 4.88; N, 9.42. Found: C, 64.57; H, 5.01; N, 9.44.

Preparation of 2,2-Bis(4-aminophenylamino)-4,4,6,6-bis[spiro-(2′,2″-dioxy-1′,1″-biphenylyl)]cyclotriphosphazene (3e). 3 (2.00 g, 3.48 mmol) was added in small portions to a melt (T = 170 °C) of 1,4-phenylenediamine (15.00 g, 0.139 mol). The reaction temperature was kept at 190 °C for 2 h, during which the color changed from orange-brown to green. The mixture was allowed to cool to room temperature and washed with hot water (4 × 100 mL). The residue was washed with MeOH until the washing solutions were nearly colorless, and the remaining microcrystalline solid was dried in vacuo. Yield: 2.20 g (88%). ^{1}H NMR (CD_3CN): δ 7.63−7.60 (m, 4 H) 7.48−7.35 (m, 8H), 7.21−7.18 (m, 4H), 6.91 (d, 4H, J = 8.7 Hz), 6.49 (d, 4H, J = 8.7 Hz), 5.65 (d, 2H, J_{PH} = 9.6 Hz), 4.18 (s, 4H). ^{31}P NMR (CD_3CN): δ 26.4 (d, J_{PP} = 69.6 Hz), 9.0 (t, J_{PP} = 69.6 Hz). Anal. Calcd for $C_{36}H_{30}N_7O_4P_3$: C, 60.26; H, 4.21; N, 13.66. Found: C, 60.21; H, 4.45; N, 13.32.

Preparation of 2,2-Bis(2-pyridylamino)-4,4,6,6-bis[spiro(*N,N*′-dimethylethylenediamino)]cyclotriphosphazene (1f). A portion of **1** (2.00 g, 5.28 mmol) was combined with solid 2-aminopyridine (11.00 g, 0.117 mol), and the mixture was heated to 185 °C for 3.5 h. The excess 2-aminopyridine was removed in vacuo on heating to 100 °C, and the residue was dissolved in 80 mL of $CHCl_3$. The organic phase was washed with water (5 × 30 mL) and subsequently dried with Na_2SO_4. The solvent was evaporated, and the remaining yellow crude product was recrystallized from toluene. Yield: 2.1 g (81%). ^{1}H NMR (CD_3Cl): δ 8.12 (d, 2H, J = 4.8 Hz), 7.42 (dd, 2H, $J_1 = J_2$ = 7.6 Hz), 7.27 (d, 2H, J = 8.2 Hz), 6.72 (dd, 2H, $J_1 = J_2$ = 6.3 Hz), 6.28 (d, 2H, J_{PH} = 9.0 Hz), 3.08 (d, 8H, J_{PH}* = 11.4 Hz), 2.50 (d, 12H, J_{PH}* = 12.0 Hz). ^{31}P NMR ($CDCl_3$) δ 29.1 (d, J_{PP} = 55.4 Hz), 6.3 (t, J_{PP} = 55.4 Hz). Anal. Calcd for $C_{18}H_{30}N_{11}P_3$: C, 43.82; H, 6.13; N, 31.22. Found: C, 43.68; H, 6.36; N, 31.16.

Preparation of 2,2-Bis(bis(2-pyridyl)amino)-4,4,6,6-bis[spiro-(2′,2″-dioxy-1′,1″-biphenylyl)]cyclotriphosphazene (3g). A sample of **3** (1.80 g, 3.13 mmol) was mixed with 2,2′-dipyridylamine (7.80 g, 45.56 mmol). The mixture was heated to 190−200 °C for 2.5 h. Excess dipyridylamine was removed in vacuo, and the remaining yellow residue was washed with 25 mL of THF. The remaining solid was dissolved in CH_2Cl_2 (80 mL), and 30 mL of water was added. NH_3(aq) was added dropwise until the mixture reached pH 8. The organic phase was separated, washed with water, and subsequently dried with Na_2SO_4. The solvent was removed under reduced pressure and the residue washed with ethyl acetate and ether. Yield: 1.8 g (68%). ^{1}H NMR (CD_3Cl) δ 8.28 (d, 4H, J = 4.0 Hz), 7.53−7.39 (m, 12H), 7.29−7.16 (m, 8H), 6.99−6.93 (m, 8H). ^{31}P NMR ($CDCl_3$) δ 25.9 (d, J_{PP} = 77.1 Hz), 10.2 (t, J_{PP} = 77.1 Hz). Anal. Calcd for $C_{44}H_{32}N_9O_4P_3$: C, 62.64; H, 3.82; N, 14.94. Found: C, 61.71; H, 3.76; N, 14.56.

Preparation of 2,2-Bis(1,4,7,10-tetraoxa-13-azacyclopentadecanyl)-4,4,6,6-bis[spiro(2′,2″-dioxy-1′,1″-biphenylyl)]cyclotriphosphazene (3h). A mixture of **3** (0.50 g, 0.87 mmol) and 1-aza-15-crown-5 (5.00 g, 22.89 mmol) was heated to 180 °C for 3 h. The reaction mixture was cooled to room temperature and poured into 80 mL of water. The resulting colorless solid was filtered and washed repeatedly with water, followed by washing with diluted aqueous ammonia, water, and methanol. The colorless solid was dried in vacuo. Yield: 0.50 g (61%). ^{1}H NMR (CD_3CN): δ 7.63−7.60 (m, 4H), 7.51−7.45 (m, 4H), 7.40−7.33 (m, 8H), 3.72 (t, 8H, 6.3 Hz), 3.59−3.56 (m, 24H), 3.26−3.22 (m, 8H). ^{31}P NMR (CD_3CN): δ 25.8 (J_{PP} = 66.7 Hz), 25.1 (J_{PP} = 66.7 Hz).[17] Anal. Calcd for $C_{44}H_{56}N_5O_{12}P_3$: C, 56.23; H, 6.01; N, 7.45. Found: C, 56.56; H, 6.26; N, 7.42.

Preparation of [{$ReCl(CO)_3$}$_2${$N_3P_3(pyNH)_2(MeNC_2H_4NMe)_2$}] (4). A sample of $N_3P_3(pyNH)_2(MeNC_2H_4NMe)_2$ (**1f**) (0.3 g, 0.61 mmol) was dissolved in 20 mL of $CHCl_3$, and [$ReCl(CH_3CN)_2(CO)_3$] (0.472 g, 1.22 mmol) was added. The mixture was refluxed for 4 h. The solvent was evaporated, and the residue was treated with cold acetone. The microcrystalline white solid was filtered and dried in vacuo. Yield: 350 mg (52%). ^{1}H NMR ($CDCl_3$): δ 9.16 (s, 2H), 8.56 (d, 2H, 5.7 Hz), 7.21 (dd, 2H, $J_1 = J_2$ = 7.8 Hz), 6.75 (dd, 2H, $J_1 = J_2$ = 7.1 Hz), 6.48 (d, 2H, 7.4 Hz), 3.52 (br s, 4H), 3.26 (br s, 4H), 2.75 (d, 6H, J_{PH}* = 12 Hz), 2.66 (d, 6H, J_{PH}* = 12 Hz). ^{31}P NMR ($CDCl_3$): δ 29.6 (d, J_{PP} = 48.5 Hz), 15.9 (t, J_{PP} = 48.5 Hz). Anal. Calcd for $Re_2Cl_2P_3O_6N_{11}C_{24}H_{30}\cdot CHCl_3$: C, 24.53; H, 2.55; N, 12.59. Found: C, 24.85; H, 2.69; N, 12.68.

Preparation of [{FeI_2}$_2${$N_3P_3(pyNH)_2(MeNC_2H_4NMe)_2$}] (5). A portion of I_2 (0.82 g, 3.24 mmol) was dissolved in 50 mL of THF, and iron powder (0.30 g, 5.37 mmol) was added. The mixture was refluxed for 1 h, and excess iron was removed with the magnetic stir bar. **1f** (0.80 g, 1.62 mmol) was added to the green solution, and the resulting mixture was refluxed for 60 min. After the mixture was cooled to room temperature, the solvent was removed in vacuo. The gray-green residue was dissolved in hot CH_3CN (25 mL), and diethyl ether (75 mL) was added to the

solution. The mixture was cooled to −30 °C. After 24 h the crystalline product was filtered and dried in vacuo. Yield: 1.42 g (79%). Anal. Calcd for $Fe_2I_4P_3N_{11}C_{18}H_{30}$: C, 19.43; H, 2.72; N, 13.85. Found: C, 19.42; H2.69; N, 13.64.

Preparation of [{$PdCl_2$}$_2${N_3P_3(pyNH)$_2$(MeNC$_2$H$_4$NMe)$_2$] (6). A portion of **1f** (0.50 g, 1.01 mmol) was dissolved in 25 mL of $CHCl_3$, and [$PdCl_2$(COD)] (0.58 g, 2.02 mmol) was added. The supension was refluxed for 2 h. During this time, [$PdCl_2$(COD)] slowly dissolved and an orange solution formed. The reaction mixture was stirred at room temperature for 12 h, and insoluble material was filtered. The solvent was removed in vacuo, and the orange residue was dissolved in a minimal amount of hot DMF (∼15 mL). Diethyl ether (60 mL) was slowly added at room temperature, and after the resulting solution was stirred for 1 h, the crystalline material was filtered, washed with diethyl ether, and dried in vacuo. Yield: 0.9 g of **6**·2DMF (89%). ^{1}H NMR ($CDCl_3$): δ 9.88 (br s, 2H), 8.42 (d, 2H, 6.0 Hz), 7.72 (dd, 2H, $J_1 = J_2 = 7.5$ Hz), 7.50 (d, 2H, 8.1 Hz), 6.96 (dd, 2H, $J_1 = J_2 = 6.5$ Hz), 3.72 (m, 4H), 3.17−3.15 (m, 2H), 3.06−2.99 (m, 2H), 2.17−2.10 (m, 12H). ^{31}P NMR ($CDCl_3$) δ 23.1 (d, $J_{PP} = 49.6$ Hz), 1.9 (t, $J_{PP} = 49.6$ Hz). Anal. Calcd for $Pd_2Cl_4P_3N_{11}C_{18}H_{30}$·2DMF: C, 28.99; H, 4.46; N, 18.31. Found: C, 29.11; C, 4.26; N, 18.23.

Preparation of [La(NO$_3$)$_3${N_3P_3(pzpy)$_2$(MeNC$_2$H$_4$NMe)$_2$}] (7). A sample of N_3P_3(pzpy)$_2$(MeNC$_2$H$_4$NMe)$_2$ (**1c**) (0.20 g, 0.34 mmol) was dissolved in 8 mL of warm MeOH and the resulting solution added to a solution of La(NO$_3$)$_3$·6H$_2$O (0.15 g, 0.34 mmol) in 5 mL of MeOH. The mixture was refluxed for 1 h and subsequently allowed to cool to room temperature. The precipitated material was filtered off, washed with MeOH, and dried in vacuo. The white solid was treated with $CHCl_3$, subsequently filtered, and redissolved in warm nitromethane. Slow addition of diethyl ether yields **7** as a colorless crystalline material. Yield: 0.22 g (70%). ^{1}H NMR (nitromethane-d_3): δ 8.86 (d, 2H, 5,2 Hz), 8.43 (d, 2H, 2.7 Hz), 8.06−7.95 (m, 4H), 7.53−7.57 (m, 2H), 7.14 (t, 2H, 3.0 Hz), 3.33−3.30 (m, 4H), 3.22−3.15 (m, 4H), 2.51−2.47 (m, 12H). ^{31}P NMR (nitromethane-d_3): δ 26.8 (d, $J_{PP} = 54.8$ Hz), 7.1 (t, $J_{PP} = 54.8$ Hz). Anal. Calcd for $LaP_3O_9N_{16}C_{24}H_{32}$: C, 31.32; H, 3.50; N, 24.35. Found: C, 31.55; H, 3.73; N, 24.18.

X-ray Structure Determination. Crystals of **3h**, **4**, **5**, **6**, and **7** suitable for X-ray structure analysis were grown by slow diffusion of pentane into a solution of **3h** in dioxane, by slow diffusion of ether into a solution of **4** in chloroform, by slow diffusion of ether into a solution of **5** in THF, by slow diffusion of ether into a solution of **6** in DMF, and by slow diffusion of ether into a solution of **7** in nitromethane, respectively. No high quality crystals could be obtained for **3h**. Several attempts were made to find the best crystal, but peak scans still showed broad peaks. The large size and flexibility of the molecule precludes a well-ordered crystal, and the above average temperature factors and disorder in the atom O5 are indicators of this (R1 [$I > 2\sigma(I)$] = 0.0972). All crystals were coated with mineral oil and mounted onto a glass fiber. X-ray data were collected using a Bruker SMART CCD area detector single-crystal diffractometer with graphite-monochromatized Mo Kα radiation ($\lambda = 0.71073$ Å) by the $\phi-\omega$ scan method at $T = 203(2)$ K.

A total of 1770 frames of intensity data were collected for each compound. Absorption corrections were applied using the SADABS[13] program. The structures were solved by direct methods and refined using full-matrix least-squares refinement on F^2 and difference Fourier synthesis using SHELXTL-PC[14] software. All non-hydrogen atoms were refined anisotropically; hydrogen atoms were included at calculated positions. Further crystallographic data for each compound are summarized in Table 3.

5. The electron density of partially occupied (∼0.75), disordered THF was removed from the unit cell using PLATON/SQUEEZE.[15] This resulted in a total of three formula units ($3C_4H_8O$) per cell being removed (117 e$^-$/cell and 785 Å^3 were found).

7. Disordered solvent (diethyl ether) is present in one void per unit cell. The contribution of the disordered solvent to the diffraction pattern was incorporated into the model using PLATON/SQUEEZE15. A total of 51 e$^-$ were found in the void (218 Å^3).

Discussion

Ligand Synthesis and Characterization. In our initial efforts to prepare cyclotriphosphazene-based bis(pyrazole) chelators, we found that these materials can be conveniently prepared in good yields by reacting readily available spirotricyclic 2,2-dichlorocyclotriphosphazenes in a melt of pyrazole.[16] In light of the strong metal-binding capabilities of these ligands, we extended this solvent-free strategy to anchor other substituents that are not only valuable candidates to bind metals but also interesting starting materials for further chemical transformations.

Among the large group of potential bidentate blocking entities to produce 2:1-site-differentiated dichlorophosphazenes, 2,2′-dihydroxybiphenyl and *N*,*N*′-dimethylethylenediamine are of particular interest since the formation of the undesired mono- or trisubstituted cyclophosphazenes can be avoided by simply controlling the stoichiometry (**3**) or temperature (**1**) of the substitution reaction. Thus, 2,2-dichloro-4,4,6,6-bis[spiro(*N*,*N*′-dimethylethylenediamino)]cyclotriphosphazene (**1**) and 2,2-dichloro-4,4,6,6-bis[spiro-(2′,2″-dioxy-1′,1″-biphenylyl)]cyclotriphosphazene (**3**) can be isolated as the sole isomers in 81% and 80% yield, respectively.[8,9] To synthesize bisspiro-type cyclophosphazenes with varying solubility and steric properties, we also targeted the synthesis of the dichlorocyclotriphosphazene with *N*,*N*′-diisopropylethylenediamine as the exocyclic side group. Following the procedure for the preparation of **1**, reaction of $N_3P_3Cl_6$ with excess *i*PrNHC$_2$H$_4$NH*i*Pr in refluxing ethereal or THF solution only yields the monosubstituted product. The failure to form **2** under moderate reaction conditions can most likely be attributed to the bulkiness of the dialkylated diamine. In contrast, **2** can readily be obtained in 71% yield if $N_3P_3Cl_6$ is allowed to react with neat *N*,*N*′-diisopropylethylenediamine at elevated temperatures (140−150 °C). It is interesting to note that no trisubstituted product has been isolated under these harsh reaction conditions. **2** can readily be separated from excess amine by adding a methanol/water mixture and can further be purified by recrystallization from heptane.

When the dichlorocyclotriphosphazenes **1**−**3** were subjected to further chlorine displacement with nucleophiles such

(13) Sheldrick, G. M. *SADABS*; University of Göttingen: Göttingen, Germany, 1996 (program for absorption corrections using Bruker CCD data).
(14) Sheldrick, G. M. *Bruker SHELXTL-PC*; University of Göttingen: Göttingen, Germany, 1997.
(15) Spek, A. L. *Acta Crystallogr.* **1990**, *A46*, C34.
(16) Harmjanz M.; Scott, B. L.; Burns, C. J. *Chem. Commun.* **2002**, 1386−1387.
(17) For the determination of ν_A, ν_B, and J_{AB} in AB_2 spin systems, see: Bovey, F. A. In *Nuclear Magnetic Resonance Spectroscopy*; Academic Press: San Diego, CA, 1988; pp 159−162.

Scheme 1

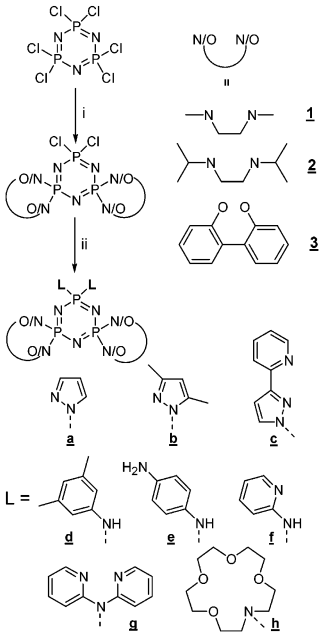

[a] Reaction conditions: (i) for **1** and **3**, see refs 8 and 9; for **2**, solvent free, excess *N*,*N*′-diisopropylethylenediamine, 150 °C, 2−3 h; (ii) solvent free, excess L, 180−200 °C, 2−7 h.

as pyrazole in refluxing toluene and in the presence of different bases, no or partial substitution was repeatedly observed. The decreased reactivity toward further substitution can be ascribed to the strong electron-donating ability and steric influence of the substituents already present on the ring. To overcome this difficulty, more drastic conditions are required to attain total chlorine replacement in an efficient way. Thus, the aminolysis of the dichlorocyclophosphazenes has been performed at 180−200 °C in a melt of selected cyclic and acyclic nitrogen-containing species L to produce 10 new cyclotriphosphazene-based ligand constructs (Scheme 1). Depending on the amine and on the difunctional geminal blocking unit, reaction times vary between 2 and 7 h. All reactions were carried out under an argon atmosphere to minimize hydrolytic and oxidative decomposition. Excess substrate can be removed by sublimation or distillation (**1a**−**3a**, **1f**, **3d**, **3g**) or simply by treating the crude product with warm ethanol (**3b**) or hot water (**1c**, **3e**, **3h**). Dissolving the residue in CH_2Cl_2 or $CHCl_3$ and washing the organic solutions with a diluted NH_4OH solution and/or water gives, after removal of the organic solvent and recrystallization, the respective ligands in 58−97% yield (Table 1).

As displayed in Scheme 1, the discussed approach provides a facile methodology to alter the nature of the metal-binding entity. As such, the number and type of donor atoms as well as the steric requirements of the ligand can easily be customized. Moreover, the constitution of the bidentate blocking unit, which contributes to the solubility and electronic characteristics of the entire ensemble, can readily be modified. Current side groups range from pyrazole (**a**) and its derivatives (**b**, **c**) to anilines (**d**, **e**) and pyridylamines (**f**, **g**). Even macrocyclic crown-type ligand systems (**h**) can readily be attached to the cyclophosphazene scaffold. In addition to the use of these materials for the complexation of transition

Table 1. Yields and ^{31}P NMR Data for the 2:1-Site-Differentiated Cyclotriphosphazenes **1a**,**c**,**f**, **2a**, and **3a**,**b**,**d**,**e**,**g**,**h**

side group	entry	yield (%)	^{31}P NMR data
pyrazole	**1a**	81	28.3 (d, J_{PP} = 58.8 Hz) 6.8 (t, J_{PP} = 58.8 Hz)
	2a	92	23.2 (d, J_{PP} = 57.1 Hz) 6.8 (t, J_{PP} = 57.1 Hz)
	3a	82	23.8 (d, J_{PP} = 80.7 Hz) 4.7 (t, J_{PP} = 80.7 Hz)
3,5-dimethylpyrazole	**3b**	58	23.7 (d, J_{PP} = 80.8 Hz) 4.5 (t, J_{PP} = 80.8 Hz)
pyridylpyrazole	**1c**	62	28.0 (d, J_{PP} = 58.8 Hz) 6.8 (t, J_{PP} = 58.8 Hz)
3,5-dimethylaniline	**3d**	97	26.2 (d, J_{PP} = 73.1 Hz) 6.5 (t, J_{PP} = 73.1 Hz)
1,4-phenylenediamine	**3e**	88	26.4 (d, J_{PP} = 69.6 Hz) 9.0 (t, J_{PP} = 69.6 Hz)
2-aminopyridine	**1f**	81	29.1 (d, J_{PP} = 55.4 Hz) 6.3 (t, J_{PP} = 55.4 Hz)
2,2′-dipyridylamine	**3g**	68	25.9 (d, J_{PP} = 77.1 Hz) 10.2 (t, J_{PP} = 77.1 Hz)
aza-15-crown-5	**3h**	61	25.8 (J_{PP} = 66.7 Hz) 25.1 (J_{PP} = 66.7 Hz)

metals, the cyclotriphosphazene **3e** (L = $NH_2C_6H_4NH$−) is an interesting candidate for further derivatizations.

All new compounds have been characterized by means of ^1H and ^{31}P NMR spectroscopy. While the different substitution patterns at the phosphorus centers of **1a**−**3g** (Table 1) give rise to one triplet (PL_2) and one doublet (P_{spiro}) in the proton-decoupled ^{31}P NMR spectra, the spectrum of the crown ether derivative **3h** exhibits a total of eight signals, typical for AB_2 systems ($J_{PP}/\Delta\nu = 0.8$).[17] In either case, these findings are in agreement with the two types of phosphorus atoms present in the cyclophosphazene ring. The ^1H NMR spectra of the dispiro phosphonitrilic imidazolidine derivatives **1a**, **1c**, and **1f** show characteristic second-order effects for the P−N−C−H protons of the bidentate alkylated ethylenediamine units. Thus, a broad absorption is evident between the signals that arise on the basis of first-order assignments. These *virtual couplings* have been observed for a variety of alkyl- and dialkylamino-substituted cyclotriphosphazenes.[18]

Figure 1 displays the solid-state structure of **3h**. Together with the core phosphorus atoms, the two stereogenic dioxybiphenyl groups constitute two seven-membered spiro rings and exhibit a twist between the phenyl groups of 40.3° and 42.1°, respectively. Although the *meso* diastereomer (*R*, *S*) of **3h** is evident in the crystal structure, a fast *R*−*S* interconversion in solution can be expected.[19] The P−O bond distances [av 1.599(6) Å] and O−P−O bond angles [av 102.0(3)°] are comparable with those found in other dioxybiphenyl *gem*-substituted cyclophosphazenes.[20] The cyclotriphosphazene skeleton is almost planar, with the largest out-of-plane displacement for N(1) of 0.12 Å.[21] Compared to the P(2/3)−N bond distances [1.575(3)−1.588(3) Å] within the phosphazene ring, the P(1)−N bond lengths [1.610(3)

(18) See, for example: (a) Krishnamurthy S. S.; Woods, M. In *Annual Reports on NMR Spectroscopy*; Webb, G. A., Ed.; Academic Press: London, 1987; Vol. 19, pp 182−183. (b) Krishnamurthy, S. S.; Sau, A. C.; Woods, M. *Adv. Inorg. Chem. Radiochem.* **1978**, *21*, 41−112. (c) Keat, R.; Ray, S. K.; Shaw, R. A. *J. Chem. Soc. A* **1965**, 7193.
(19) Amato, M. E.; Carriedo, G. A.; Alonso, F. J. G.; García-Alvarez, J. L.; Lombardo, G. M.; Pappalardo, G. C. *J. Chem. Soc., Dalton Trans.* **2002**, 3047−3053.

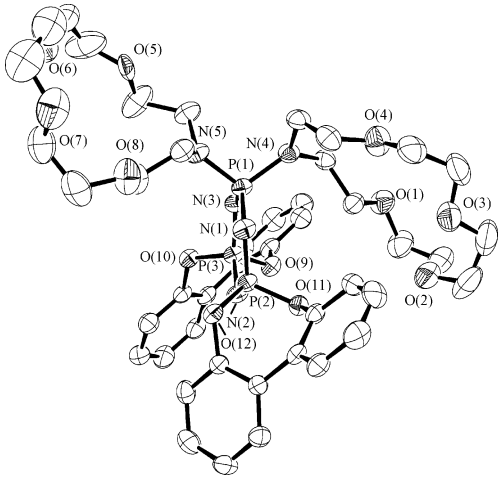

Figure 1. Molecular structure of the bis(1,4,7,10-tetraoxa-13-azacyclopentadecane)-substituted cyclotriphosphazene (**3h**). H atoms have been omitted for clarity and ellipsoids drawn at the 50% probability level.

Å] are slightly longer, which may be attributed to the strong electron-donating ability of the azacrown amino nitrogens. The overall small steric congestion at P(1) suggests a high flexibility of the two macrocycles with regard to their mutual orientation in solution, which may lead to novel sandwich-type metal complexes.

Synthesis and Characterization of Dinuclear Metal Complexes of 1f. To demonstrate and explore the activity of the prepared ligand constructs in metal complexation reactions, we have chosen to react $N_3P_3(pzpy)_2(MeNC_2H_4NMe)_2$ with $La(NO_3)_3{\cdot}6H_2O$ and **1f** with a variety of transition-metal complexes or halides {FeI_2, $[ReCl(CH_3CN)_2(CO)_3]$, $[PdCl_2(COD)]$}. On the basis of the observation that the core nitrogens of the cyclophosphazene ring most often contribute to the metal complexation,[22] **1f** is a superior candidate for the generation of dinuclear metal complexes in which each metal is simultaneously coordinated by one core nitrogen and one pyridine nitrogen. On the basis of this assumption, we reacted **1f** with excess $[ReCl(CH_3CN)_2(CO)_3]$[12] in refluxing chloroform. Evaporation of the solvent and recrystallization from cold acetone yield a white microcrystalline compound, which was spectroscopically and structurally identified as the dinuclear neutral rhenium complex **4**. As displayed in Figure 2, the solid-state structure of complex **4** possesses nearly *C*2 symmetry. The two rhenium(I) centers are being distorted octahedrally surrounded by three carbonyl carbons, one chloride, and two nitrogen donor atoms from the cyclophosphazene backbone and the adjacent pyridine, respectively. Interestingly, the coordination of two $ReCl(CO)_3$ units may lead to two isomers, in which both chloride atoms may adopt either a *cis* or a *trans* position with respect to the phosphazene plane. The solid-state structure as well as the $^1H/^{31}P$ NMR data suggests that **4** is exclusively formed as its *trans* isomer. With the carbonyl carbons in a facial arrangement, the pyridylamino-substituted phosphazene construct acts as a bidentate ligand for each rhenium atom with an average N−Re−N angle of 89.4(3)°. Both metals are slightly displaced [0.211 Å, Re(1); 0.117 Å, Re(2)] from the phosphazene ring[21] and are separated from each other by 6.484(3) Å. The six-membered chelate rings are highly distorted from planarity as evident in the torsion angles of 42.2° for P(1)−N(4)−C(1)−N(5) and 36.1° for P(1)−N(6)−C(6)−N(7). The average Re−N bond length to the phosphazene nitrogens [2.271(8) Å] is comparable to the $Re-N_{pyridine}$ bond distance [av 2.266(8) Å], and these distances are slightly elongated compared with those in the previously characterized pyridine complex $[ReCl(py)_2(CO)_3]$ [2.211(3) Å].[23] The phosphazene ring is almost planar, with the largest out-of-plane displacement for N(3) of 0.16 Å. The P−N bond distances within the ring are longest between the coordinating nitrogens [N(1), N(3)] and the ethylenediamine-substituted phosphorus atoms P(2) and P(3) [1.656(7) Å, 1.660(7) Å vs 1.557(8)−1.619(7) Å] (Table 2). This distortion likely arises from a combination of the electron-donating ability of the ethylenediamine substituents and coordination of the rhenium center by the two core nitrogen atoms. As evidenced by ^1H NMR and ^{31}P NMR ($CDCl_3$), the discussed coordination environment in the solid state remains intact and static in solution.

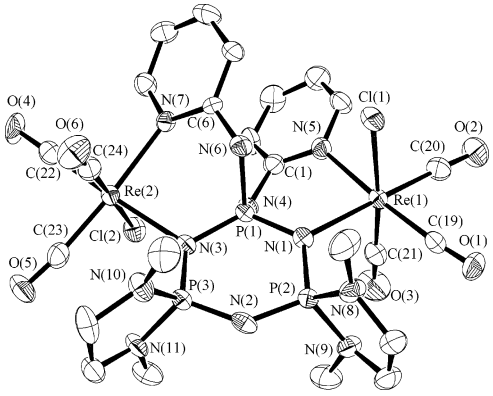

Figure 2. ORTEP diagram and partial labeling scheme of the dinuclear rhenium complex **4**. H atoms have been omitted for clarity.

Similarly, reaction of **1f** with freshly prepared FeI_2 in refluxing THF or with $[PdCl_2(COD)]$ in refluxing chloroform in a 1:2 molar ratio generates complexes of the type $[\{MX_2\}_2N_3P_3(pyNH)_2(MeNC_2H_4NMe)_2]$ [M = Fe(II), X = I (**5**); M = Pd(II), X = Cl (**6**)] as the sole isolable products. As shown in Figures 3 and 4, the di(pyridylamino)-func-

(20) Allcock, H. R.; Stein, M. T.; Stanko, J. A. *J. Am. Chem. Soc.* **1971**, *93*, 3173−3178. (b) Dez. I.; Levalois-Mitjaville, J.; Grützmacher, H.; Gramlich, V.; De Jaeger, R. *Eur. J. Inorg. Chem.* **1999**, 1673−1684. (c) Allcock, H. R.; Turner, M. L.; Visscher, K. B. *Inorg. Chem.* **1992**, *31*, 4354−4364. (d) Vij, A.; Geib, S. J.; Kirchmeier, R. L.; Shreeve, J. M. *Inorg. Chem.* **1996**, *35*, 2915−2929.

(21) Mean plane defined by P(1), P(2), and P(3).

(22) See, for example: (a) Ainscough, E. W.; Brodie, A. M.; Depree, C. V. *J. Chem. Soc., Dalton Trans.* **1999**, 4123−4124. (b) Thomas, K. R. J.; Chandrasekhar, V.; Vivekanandan, K.; Andavan, G. T. S.; Nagendran, S.; Kingsley, S.; Tiekink, E. R. T. *Inorg. Chim. Acta* **1999**, *286*, 127−133. (c) Koo, B. H.; Byun, Y.; Hong, E.; Kim, Y.; Do, Y. *Chem. Commun.* **1998**, 1227−1228. (d) Byun, Y.; Min, D.; Do, J.; Yun, H.; Do, Y. *Inorg. Chem.* **1996**, *35*, 3981−3989. (e) Diefenbach, U.; Kretschmann, M.; Stromburg, B. *Chem. Ber.* **1996**, *129*, 1573−1578. (f) Thomas, K. R. J.; Tharmaraj, P.; Chandrasekhar, V.; Bryan, C. D.; Cordes, A. W. *Inorg. Chem.* **1994**, *33*, 5382−5390.

(23) Belanger, S.; Hupp, J. T.; Stern, C. L. *Acta Crystallogr., Sect. C* **1998**, *54*, 1596−1600.

Table 2. Selected Bond Lengths (Å) for **4**−**6**

[{ReCl(CO)$_3$}$_2${N$_3$P$_3$(pyNH)$_2$(MeNC$_2$H$_4$NMe)$_2$}] (**4**)			
Re(1)−Cl(1)	2.494(2)	Re(1)−N(1)	2.280(6)
Re(1)−N(5)	2.249(8)	Re(1)−C(19)	1.927(9)
Re(1)−C(20)	1.915(9)	Re(1)−C(21)	1.903(11)
Re(2)−Cl(2)	2.503(2)	Re(2)−N(3)	2.262(7)
Re(2)−N(7)	2.283(7)	Re(2)−C(22)	1.910(8)
Re(2)−C(23)	1.911(9)	Re(2)−C(24)	1.908(11)
P(1)−N(1)	1.598(7)	P(1)−N(3)	1.619(7)
P(2)−N(1)	1.656(7)	P(2)−N(2)	1.595(7)
P(3)−N(2)	1.557(8)	P(3)−N(3)	1.660(7)
[{FeI$_2$}$_2${N$_3$P$_3$(pyNH)$_2$(MeNC$_2$H$_4$NMe)$_2$}] (**5**)			
Fe(1)−I(1)	2.5944(11)	Fe(1)−I(2)	2.6276(12)
Fe(1)−N(1)	2.095(4)	Fe(1)−N(5)	2.167(5)
Fe(2)−I(3)	2.6187(11)	Fe(2)−I(4)	2.5953(11)
Fe(2)−N(3)	2.071(4)	Fe(2)−N(7)	2.137(5)
P(1)−N(1)	1.608(5)	P(1)−N(3)	1.600(5)
P(2)−N(1)	1.651(5)	P(2)−N(2)	1.583(5)
P(3)−N(2)	1.586(5)	P(3)−N(3)	1.654(5)
[{PdCl$_2$}$_2${N$_3$P$_3$(pyNH)$_2$(MeNC$_2$H$_4$NMe)$_2$}] (**6**)			
Pd(1)−N(1)	2.050(6)	Pd(1)−N(5)	2.051(7)
Pd(1)−Cl(1)	2.292(2)	Pd(1)−Cl(2)	2.300(2)
Pd(2)−N(3)	2.083(5)	Pd(2)−N(7)	2.027(6)
Pd(2)−Cl(3)	2.281(2)	Pd(2)−Cl(4)	2.291(2)
P(1)−N(1)	1.614(6)	P(1)−N(3)	1.608(6)
P(2)−N(1)	1.649(6)	P(2)−N(2)	1.575(6)
P(3)−N(2)	1.589(6)	P(3)−N(3)	1.655(6)

tionalized cyclophosphazene construct acts as a bis-bidentate ligand, which again provides two N donor atoms from the pyridyl rings and two from the cyclophosphazene backbone. The individual metal centers are separated from each other by 5.99 Å (**5**) and 6.04 Å (**6**), respectively.

The geometry about the iron atoms in the dinuclear complex **5** is best described as pseudotetrahedral with bite angles of the ligand of 97.90(18)° and 97.96(18)° and N−Fe−I angles ranging from 102.24(13)° to 121.67(13)°. The degree of distortion can also be seen in the deviations of the dihedral angles from 90°, defined by the two planes N(1), N(5), Fe(1) [N(3), N(7), Fe(2)] and I(1), I(2), Fe(1) [I(3), I(4), Fe(2)], respectively (86.0°, 85.8°). Interestingly, the Fe−$N_{phosphazene}$ [2.095(4), 2.071(4)] bond lengths are substantially shorter than the Fe−$N_{pyridine}$ [2.167(5), 2.137(5)] bond lengths (Table 2). As such, the Fe−$N_{phosphazene}$ distances rather resemble those in the FeI_2 complex of the strong bidentate donor ligand bis(tetramethylguanidino)propane (btmgp) [av 2.039(3) Å],[24] while the Fe−$N_{pyridine}$ distances are comparable with those in the diamino complex [FeI_2(tmeda)] [av 2.14(2) Å].[25] This again illustrates the donor strength of the cyclophosphazene nitrogen atoms and indicates that the cyclophosphazene nitrogen atoms must be taken into consideration for complex design and synthetic strategies. As observed in the solid-state structure of **4**, the coordination of the Fe centers by the core nitrogens slightly affects the structural parameters within the phosphazene ring, and the observed pattern of the P−N bond lengths distribution in **5** matches that in **4**.

In the solid-state structure of **6**, the two palladium atoms adopt a distorted square planar coordination environment with average N−Pd−N angles of 85.2(2)° and average Cl−Pd−Cl angles of 91.47(9)°. In contrast to the structures of **4** and **5**, in which the two pyridyl entities are aligned in an almost parallel fashion, the pyridyl groups in **6** are pointing away from each other, forcing the $PdCl_2N_2$ planes to adopt a nearly perpendicular orientation with respect to the cyclophosphazene ring [66°, Pd(2); 75°, Pd(1)]. In analogy to **4**, the Pd−$N_{phosphazene}$ bond lengths [2.050(6) Å, 2.083(5) Å] are comparable with the Pd−$N_{pyridine}$ bond distances [2.051(7) Å, 2.027(6) Å] (Table 2). Apparently, no clear trend between the M−$N_{pyridine}$ and M−$N_{phosphazene}$ bond lengths is evident in **4**−**6**, but the discussed discrepancies may arise from the respective steric and electronic constraints with regard to metal to $N_{phosphazene}$ interactions. The P−N bond lengths within the phosphazene scaffold in **6** range from 1.575(6) to 1.655(6) Å, and the bond length distribution is strikingly similar to that of **4** and **5**.

The formation of the dinuclear complexes **4** and **6** can also be monitored by ^{31}P NMR. In addition to the pyridylamino groups at P(1) (Figures 2 and 4), this phosphorus atom is surrounded by two metal-coordinating core nitrogens. Compared to the free ligand [δ = 29.1 (d), 6.3 (t) ppm], metalation results in a significant shift of the signal pattern (triplet) of P(1). Although metal binding by the cyclophosphazene nitrogen atoms suggests an increased deshielding at P(1), the expected downfield shift of the triplet can only be observed for **4** (δ = 15.9 ppm), while the spectrum of **6** displayed a noticeable upfield shift (δ = 1.9 ppm). The ^{1}H NMR spectrum of **4** establishes the dinuclear nature of this complex in solution. The given coordination geometry in **4**, with the Cl and CO ligands in the *trans* position gives rise to two nonequivalent methyl and methylene groups of the bidentate *N*,*N*′-dimethylethylenediamine substituents. As observed for the ligands **1a**, **1c**, and **1f**, characteristic second-order effects for the P−N−C−H protons are evident. Although the geometry in the Pd complex **6** suggests a similar signal pattern, a splitting of the ^{1}H NMR signals of the *N*,*N*′-dimethylethylenediamine methyl groups into two distinct ^{31}P-coupled signals can only be observed at higher temperatures. At room temperature, however, the ^{1}H NMR shows a multiplet for the methyl groups and three multiplets for the methylene hydrogens in a 2:1:1 ratio. These findings suggest a solution dynamic behavior of **6** that may originate in a flexing of the two pyridylamino groups between a nearly parallel position and an arrangement in which both pyridyl groups are pointing away from each other (Figure 4). This motion may, to some extent, also involve cleavage of the Pd−$N_{phosphazene}$ bonds.

To investigate potential electronic communication between the metal centers by way of the ligand π-system, the electrochemical properties of the free ligand **1f** and the corresponding redox-active diiron complex **5** were examined. The cyclic voltammogram of **5** in benzonitrile is shown in Figure 6. While the free ligand was found to be redox inactive between +1.04 and −2.20 V vs [$FeCp_2$] (benzonitrile), the voltammogram of **5** displays two distinct oxidation waves with a peak potential at E_{Pox} = +0.34 V and E_{Pox} = +0.59 V vs [$FeCp_2$], respectively. Although this result would be in agreement with the successive oxidative formation of

(24) Pohl, S.; Harmjanz, M.; Schneider, J.; Saak, W.; Henkel, G. *J. Chem. Soc., Dalton Trans.* **2000**, 3473−3479.
(25) Calderazzo, F.; Englert, U.; Pampaloni, G.; Vanni, E. *C. R. Acad. Sci., Ser. IIc* **1999**, *2*, 311−319.

Table 3. Crystallographic Data for **1h**, **4**·$CHCl_3$, **5**·0.75THF, **6**·2DMF, and **7**·0.5Et_2O

	3h	**4**·$CHCL_3$	**5**·0.75THF	**6**·2DMF	**7**·0.5Et_2O
empirical formula	$P_3O_{12}N_5C_{44}H_{56}$	$Re_2P_3Cl_5O_6N_{11}C_{25}H_{31}$	$Fe_2I_4P_3O_{0.75}N_{11}C_{21}H_{36}$	$Pd_2Cl_4P_3O_2N_{13}C_{24}H_{44}$	$LaP_3O_{9.5}N_{16}C_{26}H_{37}$
M_r	939.85	1224.17	1166.82	994.23	957.54
T/K	203(2)	203(2)	203(2)	203(2)	203(2)
cryst syst	monoclinic	triclinic	monoclinic	monoclinic	triclinic
space group	$P2_1/c$	$P\bar{1}$	$P2_1/n$	$C2/c$	$P\bar{1}$
a/Å	22.214(9)	11.225(3)	14.114(4)	20.712(7)	9.6291(13)
b/Å	11.700(4)	11.484(3)	16.681(5)	10.281(3)	11.8931(18)
c/Å	18.977(8)	17.683(5)	16.772(5)	38.104(11)	18.220(3)
α/deg		80.303(4)			76.506(2)
β/deg	111.527(7)	85.976(4)	91.431(6)	96.866(9)	81.191(3)
γ/deg		62.316(4)			78.136(2)
V/Å^3	4588(3)	1989.6(8)	3948(2)	8055(4)	1973.4(5)
Z	4	2	4	8	2
D_c/g cm^{-3}	1.361	2.043	1.963	1.640	1.611
μ(Mo Kα)/cm^{-1}	1.97	65.88	40.16	13.19	12.74
no. of reflns collected	28104	12850	24663	25211	10925
no. of unique reflns	8284	6655	7174	7407	5356
no. of refined params	586	469	344	433	478
GOF on F^2	1.817	1.145	1.131	1.257	1.036
R1[a] [$I > 2\sigma(I)$]	0.0972	0.0472	0.0435	0.0644	0.0530
wR2[b]	0.1802	0.1237	0.0969	0.1461	0.1361

[a] $R1 = \sum||F_o| - |F_c| / \sum|F_o|$. [b] $wR2 = [\sum[w(F_o^2 - F_c^2)^2]/[\sum w(F_o^2)^2]]^{1/2}$; $w = 1/[\sigma^2(F_o)^2 + (xP)^2 + yP]$, where $P = (F_o^2 + 2F_c^2)/3$.

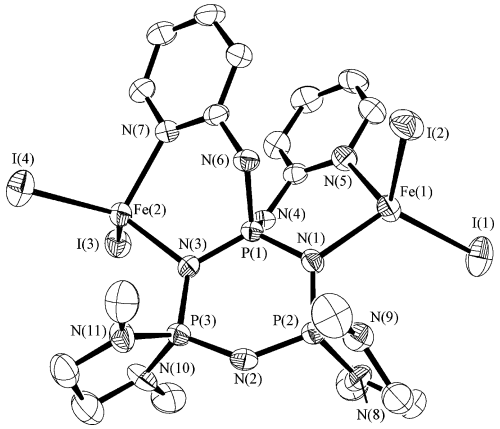

Figure 3. Molecular structure and partial labeling scheme of the dinuclear iron complex **5**. All hydrogen atoms have been omitted for clarity.

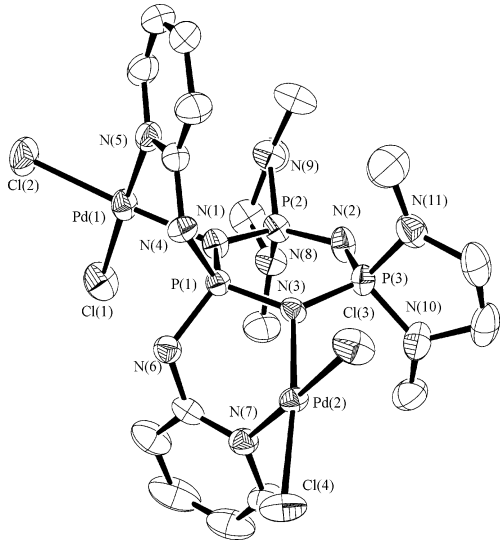

Figure 4. ORTEP diagram and partial labeling scheme of the dinuclear complex **6**. H atoms have been omitted for clarity.

the corresponding Fe^{2+}/Fe^{3+} and Fe^{3+}/Fe^{3+} dinuclear species, we found that the cyclic voltammogram of the analogous dinuclear $FeCl_2$ complex exhibits only one irreversible oxidation wave at $E_{Pox} = +0.50$ V vs $[FeCp_2]$.[26] Moreover, the cyclic voltammogram of the mononuclear FeI_2 species $[FeI_2\{N_3P_3(3,5\text{-}Ph_2pz)_2(MeNC_2H_4NMe)_2\}]$[26] shows a redox pattern closely related to that of **5**. On the basis of these findings, the second oxidation observed for **5** might involve the oxidation of the iodide coligands.

Lanthanum Complex 7. Pyrazolylpyridine is a commonly used component of many elaborate ligand architectures. Related to the well-known bis- and tris(pyrazolyl)borate ligands, terdentate chelating (pyrazolylpyridyl)borate analogues are among the most widely investigated pyrazolylpyridine-based ligand systems.[27] The small steric congestion at the apical borate headgroup, however, allows for the free rotation of the pyrazolylpyridine units, which often results in the formation of bridged, multinuclear metal complexes.[27] Given the steric control that can be built into the phosphazene construct, 2,2-bis(3-(2-pyridyl)pyrazolyl)cyclotriphosphazenes such as **1c** may improve the ligation properties and significantly reduce the tendency to form metal complexes with bridging coordination modes. In our efforts to explore the coordination properties of **1c**, we reacted this ligand in a 1:1 molar ratio with $La(NO_3)_3 \cdot 6H_2O$ in refluxing methanol. The resulting solid has been structurally and spectroscopically identified as the mononuclear complex **7**. The 1:1 stoichiometry of the product is different from that of the reaction of the anionic ligand bis(pyrazolylpyridyl)borate (Bp^{Py}) with various trivalent lanthanide ions. This reaction typically yields mononuclear complexes of the type $[Ln(Bp^{Py})_2(NO_3)]$[28]

(26) Harmjanz, M.; Burns, C. J. Unpublished results.

(27) Ward, M. D.; McCleverty, J. A.; Jeffery, J. C. *Coord. Chem. Rev.* **2001**, *222*, 251−272.

(28) (a) Bardwell, D. A.; Jeffery, J. C.; Jones, P. L.; McCleverty, J. A.; Psillakis, E.; Reeves, Z.; Ward, M. D. *J. Chem. Soc., Dalton Trans.* **1997**, 2079−2086. (b) Armaroli, N.; Accorsi, G.; Barigelletti, F.; Couchman, S. M.; Fleming, J. S.; Harden, N. C.; Jeffery, J. C.; Mann, K. L. V.; McCleverty, J. A.; Rees, L. H.; Starling, S. R.; Ward, M. D. *Inorg. Chem.* **1999**, *38*, 5769−5776.

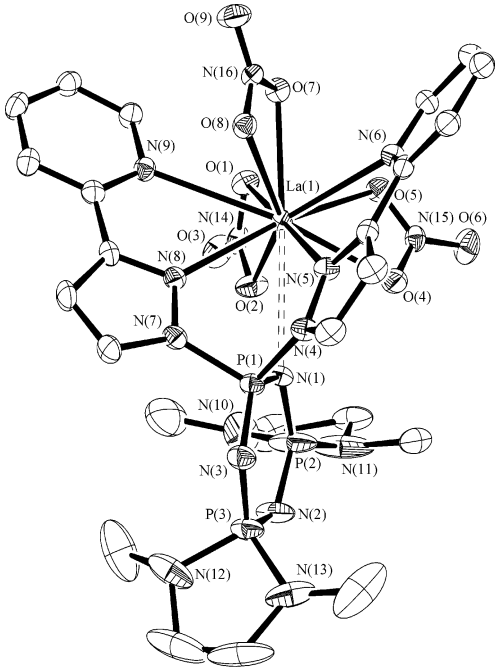

Figure 5. ORTEP diagram (ellipsoids drawn at the 30% probability level) and partial labeling scheme of the mononuclear complex **7**. H atoms have been omitted for clarity. Selected bond lengths (Å): La(1)−O(1), 2.700(5); La(1)−O(2), 2.544(6); La(1)−O(4), 2.584(5); La(1)−O(5), 2.626(5); La(1)−O(7), 2.563(5); La(1)−O(8), 2.626(5); La(1)−N(5), 2.667(6); La(1)−N(6), 2.837(6); La(1)−N(8), 2.678(5); La(1)−N(9), 2.897(6).

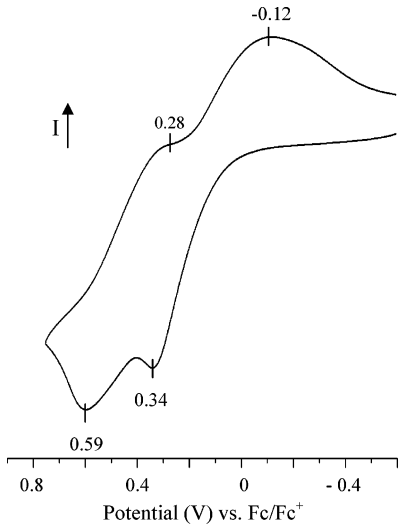

Figure 6. Cyclic voltammogram of complex **5** in benzonitrile solution. Data were recorded with a Pt working electrode, a Pt wire counter electrode, a silver wire pseudo reference electrode, an electrolyte (nBu$_4$N$^+$PF$_6^-$) concentration of 0.1 M, and a scan rate of 100 mV/s. Ferrocene was used as a standard.

in which two Bp^{Py} units are encapsulating one central metal ion. As displayed in Figure 5, **1c** acts as a tetradentate ligand, with the two bidentate pyrazolylpyridine arms coordinated to the La(III) center. In addition, the central metal ion is surrounded by three nitrates with average metal−oxygen distances of 2.61(6) Å, yielding an overall coordination number of 10. A close contact exists between the metal ion and one core nitrogen [La(1)−N(1), 3.092 Å]. The pyridine and the pyrazole rings of the respective N,N′-bidentate arms are nearly coplanar. The inherent rigidity of the diverging chelating pyrazolylpyridine substituents results in significantly shorter La−N$_{pz}$ bond distances [2.67(1) Å] in comparison to the La−N$_{py}$ bond lengths [2.87(3) Å]. These geometric constraints can also be seen in the notably dissimilar N−La−N angles [N$_{pz}$−La−N$_{pz}$, 70.64(18)°; N$_{py}$−La−N$_{py}$, 125.59(16)°]. As has been observed for **4** and **5**, the P−N bond distances within the ring are longest between N(1)/N(3) and the ethylenediamine-substituted phosphorus atoms. Apparently, the weak interaction of N(1) with La has negligible impact on the geometry within the cyclophosphazene backbone. It is important to note that this interaction is not evident in the room-temperature ^{31}P solution NMR (nitromethane-d_3). As such, the ^{31}P NMR shows only one doublet and one triplet, consistent with an AX$_2$ pattern.

Concluding Remarks

In conclusion, on the basis of the cyclotriphosphazene backbone, a straightforward route was developed to prepare highly flexible ligand systems. The solvent-free methodology readily provides many variables that can be incorporated into the ligand constructs. Given the numerous combinations of exocyclic side groups and metal-binding sites, the described approach provides an efficient protocol to customize the reactivity and solubility of the ligand architectures. In addition, this synthetic approach may be adapted as a means to introduce other side groups. The prepared ligands can be considered as neutral alternatives (e.g., **1a**−**3a**) to existing anionic ligand systems such as tris(pyrazolyl)borate and may serve as model compounds for the metal-binding sites of related high molecular weight polyphosphazenes. Mono- and dinuclear metal complexes have been successfully prepared to demonstrate and explore the activity of selected ligand constructs in metal complexation reactions.

Promising studies addressing the generation of polyphosphazenes with closely related substitution patterns are currently in progress.

Acknowledgment. We acknowledge the LANL Laboratory Directed Research and Development Program for support. M.H. is the recipient of a Director's postdoctoral fellowship at LANL.

Supporting Information Available: Crystallographic data in CIF format. This material is available free of charge via the Internet at http://pubs.acs.org.

IC034990B